


# Impact of Water Mixing and Ice Formation on the Warming of Lake Superior: A Model-guided Mechanism Study

Xinyu Ye,<sup>1</sup> Eric J. Anderson,<sup>2</sup> Philip Y. Chu,<sup>2</sup> Chenfu Huang,<sup>1</sup> Pengfei Xue <sup>1\*</sup>

<sup>1</sup>Great Lakes Research Center and Department of Civil and Environmental Engineering, Michigan Technological University, Houghton, Michigan

<sup>2</sup>NOAA - Great Lakes Environmental Research Laboratory, Ann Arbor, Michigan

## Abstract

The Laurentian Great Lakes are one of the most prominent hotspots for the study of climate change induced lake warming. Warming trends in large, deep lakes, which are often inferred by the observations of lake surface temperature (LST) in most studies, are strongly linked to the total lake heat content. In this study, we use a 3D hydrodynamic model to examine the nonlinear processes of water mixing and ice formation that cause changes in lake heat content and further variation of LST. With a focus on mechanism study, a series of process-oriented experiments is carried out to understand the interactions among these processes and their relative importance to the lake heat budget. Using this hydrodynamic model, we estimate the lake heat content by integrating over the entire 3D volume. Our analysis reveals that (1) Heat content trends do not necessarily follow (can even be opposed to) trends in LST. Hence, using LST as a warming indicator can be problematic; (2) vertical mixing in water column may play a more important role in regulating lake warming than traditionally expected. Changes in the water mixing pattern can have a prolonged effect on the thermal structure; (3) Ice albedo feedback, even in cold winters, has little impact on lake thermal structure, and its influence on lake warming may have been overestimated. Our results indicate that climate change will not only affect the air-lake energy exchange but can also alter lake internal dynamics, therefore, the lake's response to a changing climate may vary with time.

Climate change induced lake warming in both tropical and high latitude lakes has been investigated recently by numerous studies (Burnett et al. 2003; Livingstone 2003; O'Reilly et al. 2003; Verburg et al. 2003; Coats et al. 2006; Vollmer et al. 2008; Adrian 2009; Arvola et al. 2009; Schneider et al. 2009; Schneider and Hook 2010; Fink et al. 2014; Grone-wold et al., 2015). For example, O'Reilly et al. (2015) found that warming lakes are geographically distributed by using worldwide synthesis of in situ and satellite-derived lake data, revealing that the warming rate of seasonally ice-covered lakes is 0.72°C per decade while ice-free lakes are experiencing 0.53°C per decade from 1985 to 2009.

It has been observed that east-central North America, including the Laurentian Great Lakes, is one of the most prominent hotspots where lake surfaces have warmed more rapidly than the ambient air during the summer (Austin and Colman 2007; Lenters et al. 2013). A warming trend of lake

surface temperature (LST) in the Laurentian Great Lakes in the last century was reported by McCormick and Fahnenstiel (1999). Austin and Colman (2008) estimated an average summer (July, August, and September) LST warming rate of ~ 0.278°C per decade over the last century, with a dramatic increase up to 0.118°C per year after the 1980s using the off-shore buoy data. In addition, similar results from 1986 to 2002 were reported by Dobiesz and Lester (2009), estimating that LST of Lakes Huron and Ontario during August have been rising at annual rates of 0.084°C and 0.048°C, respectively, while the trend for Lake Erie, the shallowest of the Great Lakes, was smaller and insignificant.

While it is suggested that the mechanism for summer warming in the shallow lakes, such as Lake Erie, is due to a rapid response of the lakes to synchronous increases in solar radiation and air temperature during the summer (Adrian et al. 1999; Gerten and Adrian 2000; Livingstone 2003; Straile et al. 2003; Piccolroaz et al. 2014), the mechanism responsible for large, deep lakes (Gorham 1964; Robertson and Ragotzkie 1990; Mazumder and Taylor 1994) such as Lake Superior is different. Due to the much larger heat capacity and thermal inertia, the deeper lakes integrate the effects of increasing air temperature over longer periods of time (Verburg et al. 2003; Arvola 2009; Piccolroaz et al. 2015; Zhong et al. 2016). For

\*Correspondence: pexue@mtu.edu

This is an open access article under the terms of the Creative Commons Attribution-NonCommercial-NoDerivs License, which permits use and distribution in any medium, provided the original work is properly cited, the use is non-commercial and no modifications or adaptations are made.

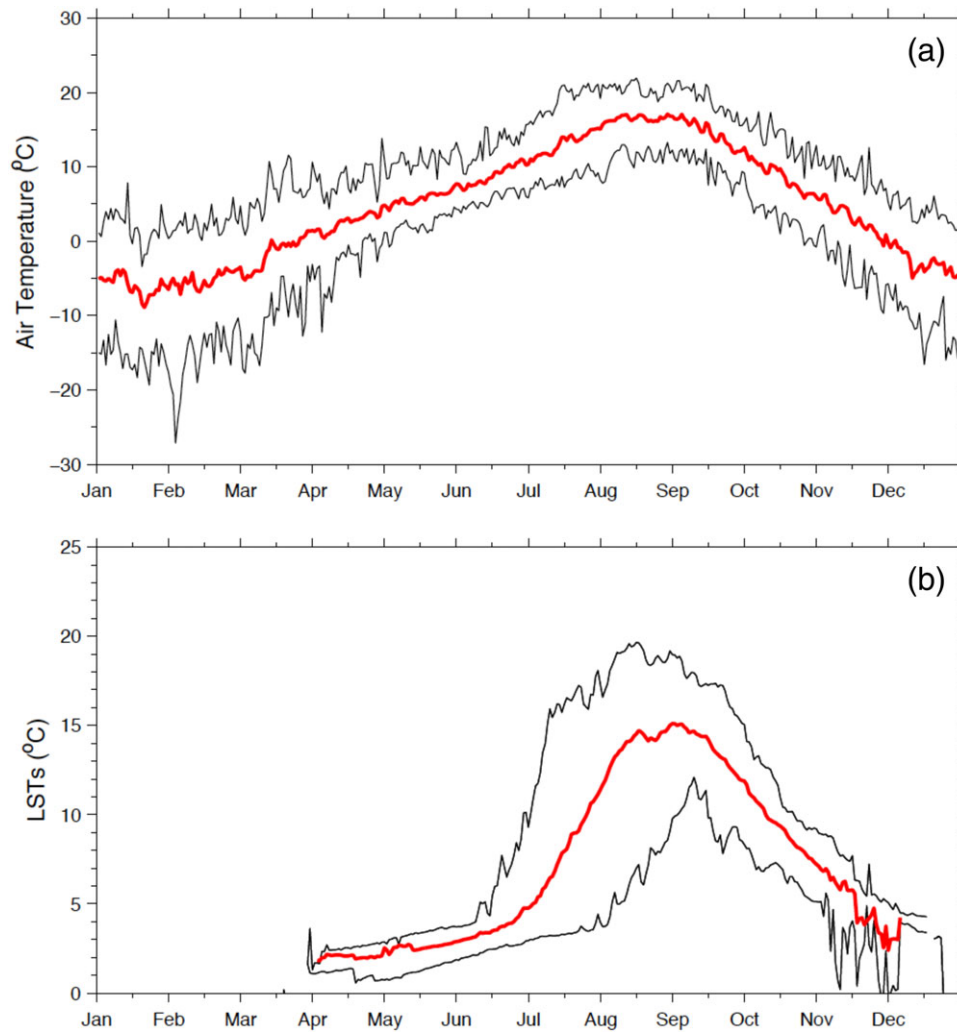


**Fig. 1.** Twenty-year climatology (1995–2013) envelopes observed near-surface air temperatures **(a)** for stations 45001, 45004, 45006, DISW3 and PILM4 and LSTs **(b)** for stations 45001, 45004, and 45006 with mean values (red lines) in Lake Superior. See Fig. 2 for buoy locations.

example, Fig. 1 presents 20-yr climatologies (1995–2013) of the observed air temperature and LST in Lake Superior. For the air temperature over Lake Superior, the largest variability with a range of  $\sim 15\text{--}20^\circ\text{C}$  occurs during the winter time, and much smaller variability ( $\sim 8\%$ ) is shown during the summer. In contrast, due to the large thermal inertia, strong interannual and intra-lake variability of the LST is observed during summer time with a fluctuation range of  $\sim 6\text{--}20^\circ\text{C}$  in mid-August. This phenomenon clearly shows the LST variation of Lake Superior does not solely follow changes in air temperature. For Lake Superior, the atmospheric condition is apparently not the only factor that controls changes in LST. Internal lake processes and heat transfer must also play very important roles in regulating lake warming in Lake Superior.

It is no question that the combination of winter lake inverse stratification, ice-coverage, solar radiation, onset of spring stratification, and air temperature influences lake heat absorption and affects lake surface warming during the

subsequent summer (Van Cleave et al. 2014; Piccolroaz et al. 2014, 2015; Mason et al. 2016; Sugiyama et al. 2018), which results in significant spatial and temporal variation in warming patterns within and across the Great Lakes (Mason et al. 2016). However, there is no consensus regarding how these mechanisms control the LST warming, and the lake–ice–atmosphere interaction allows for the formation of multiple climate regimes with prolonged impact on lake warming (Sugiyama et al. 2018). For example, Austin and Colman (2007) suggested that winter ice cover seems to play an important role in determining subsequent summer LST in Lake Superior with a majority of the interannual variability in the summer LST explained by the previous winter’s ice coverage. Their study also suggested that ice coverage changes the dynamics of thermal exchange primarily due to ice albedo effect because ice significantly increases the surface albedo, reducing the net shortwave radiation absorbed by the lake. As such, lake warming reduces the ice concentration and further

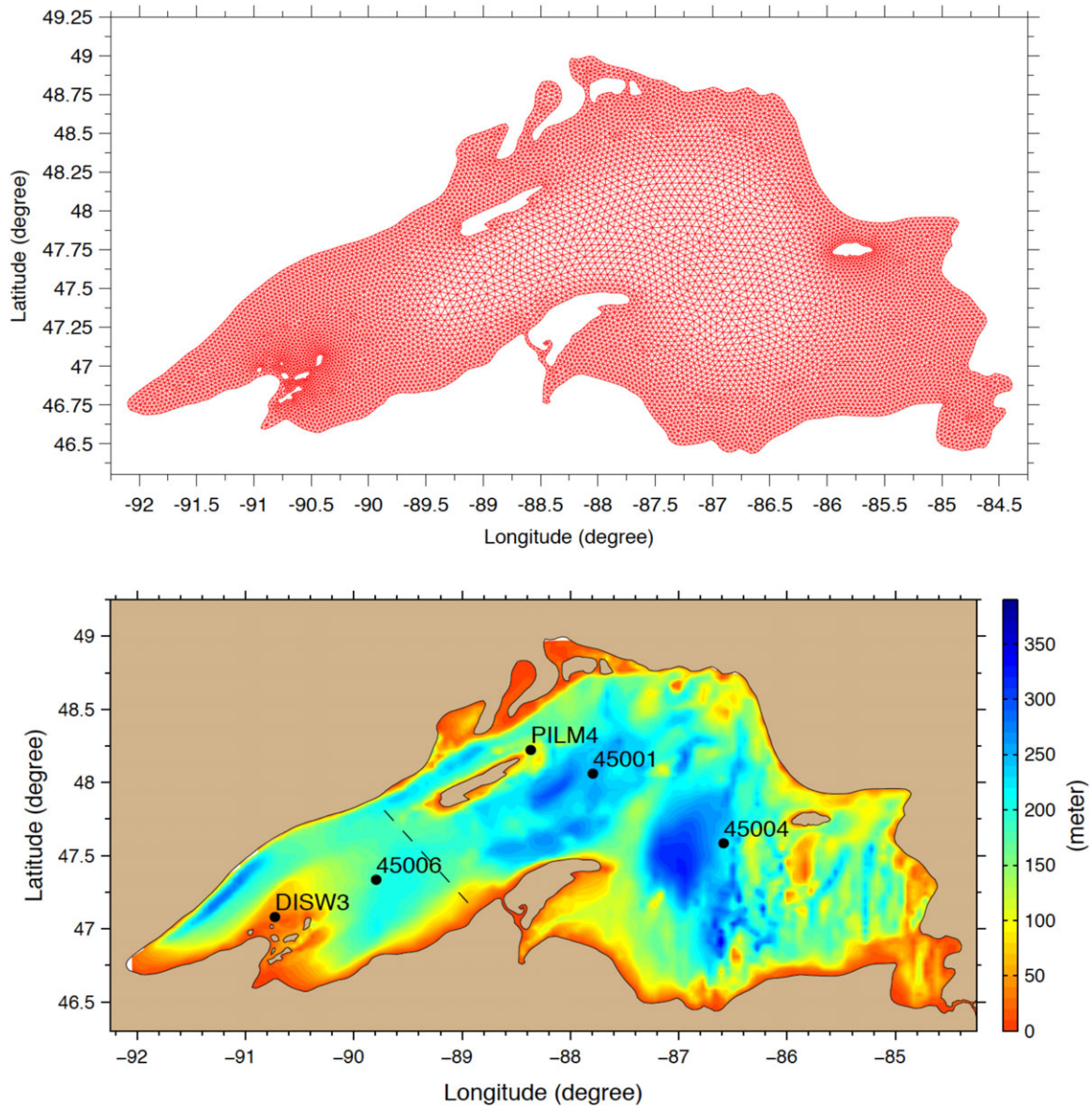


**Fig. 2.** FVCOM model mesh with unstructured triangular grids in the upper panel, and the bathymetry of Lake Superior in the lower panel. The buoy stations are marked as black dots, a reference cross-section is denoted by a black dashed line.

increases the solar heat input to the lake, leading to more rapid warming. Schneider and Hook (2010) pointed out that changes in insolation, ice cover, and other factors are important contributing factors, and declining ice cover is not a prerequisite for accelerated summertime lake warming (Schneider et al. 2009; Zhong et al. 2016). Furthermore, Zhong et al. (2016) concluded that antecedent winter ice cover plays a minor role in changes in the accelerated warming of Lake Superior. Mild winter conditions, together with increased solar radiation, air temperature during spring, causes an earlier onset and increased strength of springtime stratification (Scheffer et al. 2001; Verburg et al. 2003; Arvola 2009; Piccolroaz et al. 2015), resulting in enhanced heat absorption by

surface water and thereby contributing to lake surface warming (Piccolroaz et al. 2015; Zhong et al. 2016). Hence, the question of how the heat transfer and ice coverage influence the LST remains unclear.

Furthermore, lake warming, which is inferred by LST observation in most of the previous studies, is in fact strongly linked to the total heat content in the lake through the winter to the following summer. Ecologically, understanding the change in lake heat content is much more important than LST (Lynch et al. 2010; Collingsworth et al. 2017). Even relatively small changes in the thermal characteristic of lakes can cause major shifts in the aquatic ecosystem such as the phytoplankton, bacterioplankton, and zooplankton populations and

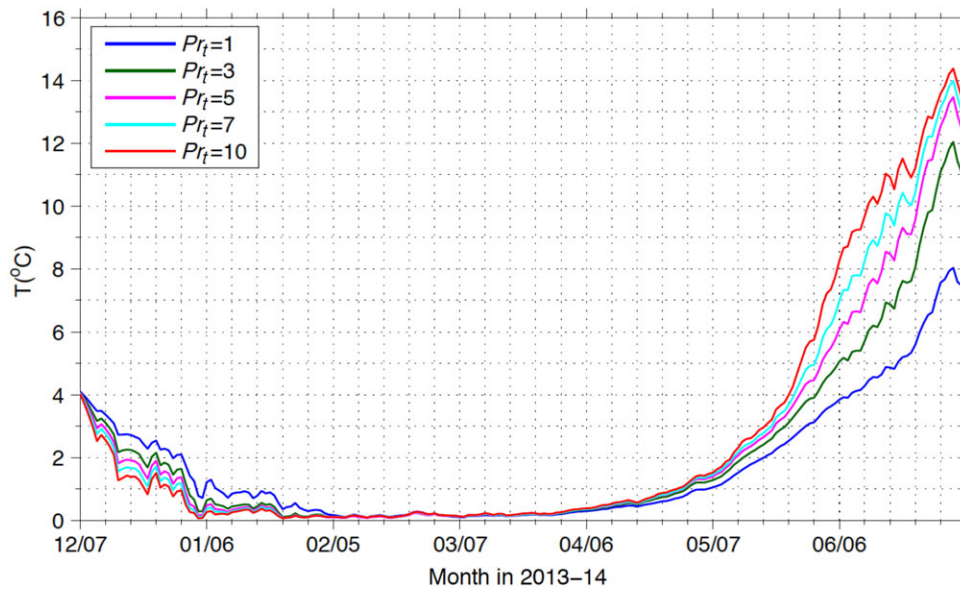


**Fig. 3.** Model simulated lake-wide mean LST with different turbulent Prandtl number parameterization for the sensitivity test.

associated metabolic processes (Tulonen et al. 1994; Drinkwater 2003; Adrian 2009; Arvola 2009; Lynch et al. 2010; Butcher et al. 2015; Collingsworth et al. 2017). For example, it has been reported that the lake regime shifts have influenced the structure of species-dependent cyanobacteria in western countries (Wagner and Adrian 2009) and even a 1°C temperature drop could decrease the critical fish density by ~ 5% in a sample of 71 shallow Dutch lakes (Scheffer et al. 2001). Therefore, analyzing the factors that influence heat content is critical to understanding the ecosystem. Ultimately, it is vital to calculate the heat content in the most comprehensive way. However, limited in situ observations do not allow us to estimate the lake heat content change accurately. That’s partly why LST has been used more often as an indicator of lake warming in response to climate change because much more in situ and remotely sensed data are readily available at the lake surface.

In a changing climate, the direct impact of change in atmospheric heat flux into the lake is often extensively studied and used to project the lake warming rate. However, the lake mixing plays an important role in transferring heat mechanically downward. As a result, a thermocline can intensify or diminish in response to the mixing processes and significantly affect the heat storage pattern and the lake warming trend (Butcher et al. 2015). Warming of surface water in the last three decades as well as changes in the wind pattern have altered the strength of thermal stratification, which leads to changes in water mixing and water temperature at depth in some large, deep lakes (Desai et al. 2009; Bennington et al. 2010; Butcher et al. 2015). Therefore, it is critical to understand the mixing process that determines the nonlinear relationship between LST, surface heat fluxes, and total heat content in the context of lake warming.

In this paper, we use a 3D hydrodynamic model to examine the nonlinear processes of water mixing and ice

formation that cause deviations in lake heat content and further variation of LST in the following year. A series of process-oriented numerical experiments were carried out to identify and quantify the interactions of the processes and their relative contribution to the lake heat budget with specific goals of (1) establishing the heat budget of Lake Superior accounting for heat storage change over the entire lake in a 3D model, (2) understanding changes in the thermocline and thermal stability of the lake in response to water mixing and ice formation, (3) examining the response of LST and heat content to the variability of water mixing, and (4) quantifying the competitive role of ice albedo feedback and ice insulation effects.

The remaining sections of this paper are organized as follows: Model configuration and design of numerical experiments are described in “Model description and design of the experiments” section. The results and discussion of each experiment are presented in “Results and discussion” section. A summary of findings is concluded in “Conclusion” section.

## Model description and design of the experiments

### Hydrodynamic model

Finite Volume Community Ocean Model (FVCOM) (Chen et al. 2006) is used in this study, which is an unstructured-grid, finite-volume, three-dimensional (3D), primitive equation ocean model. FVCOM’s unstructured-grid feature allows for flexible geometrical fitting and local topography refinement, which has proven successful for research and applications to estuaries, coastal oceans, and Lakes (Xue et al. 2009, 2015, 2017; Anderson and Schwab 2013; Beardsley et al. 2013; Fujisaki-Manome et al. 2017; Safaie et al. 2017). The horizontal resolution of the model grids varies from ~



**Table 1.** The configuration of numerical experiments.

Experiment #	Vertical Prandtl number	Ice albedo
C1-1	1	Dynamics calculated
C1-2	3, 5, 7, 10	Dynamics calculated
C2-1	1	0.7
C2-2	1	0.06

1 km near the coast to 5 km in the offshore regions of the lake (Fig. 2). The model is configured with 40 sigma layers to provide a vertical resolution of  $< 1$  m for nearshore waters and  $\sim 2$ –5 m in most of the offshore regions of the lake. The Mellor-Yamada level 2.5 (MY25) turbulence closure model (Mellor and Yamada 1982) is used for simulating vertical mixing processes, which includes a set of prognostic equations for turbulent kinetic energy and a length-scale-related parameter to calculate eddy viscosities and vertical diffusivities. The horizontal diffusivity is calculated using the Smagorinsky numerical formulation (Smagorinsky 1963), determined by the horizontal velocity shear as well as the model grid resolution.

#### Vertical mixing and turbulent Prandtl number

The turbulent Prandtl number ( $Pr_t$ ), the ratio of eddy viscosity ( $K_M$ ) and eddy diffusivity ( $K_H$ ), determines the relative efficiency of the vertical turbulent exchanges of momentum and heat. In a neutral environment, it is usually found that the eddy coefficients of heat and momentum are approximately equivalent ( $Pr_t \sim 1$ ). The presence of stable stratification reduces the vertical transport of both heat and momentum. In general, the eddy diffusivity  $K_H$  decreases faster than the eddy viscosity  $K_M$  with increasing stratification, thus increasing the  $Pr_t$  in a stable environment.

In the ocean and the large lakes, the  $Pr_t$  can vary to a great extent. For example, Muench et al. (2009) estimated the  $Pr_t$  value of 1.5 and 4.2 at two CTD measurement sites in the Ross Sea continental shelf. Goodman and Levine (2003) showed that the  $Pr_t$  varies between 2 and 8 in the Narragansett Bay, Rhode Island using Autonomous Underwater Vehicle (AUV) data. Previous modeling studies have shown that the  $Pr_t$  variation in a vertical mixing scheme can significantly affect the simulation results (Noh et al. 2005; Elliott and Venayagamoorthy 2011). Dunckley et al. (2012) used  $Pr_t = 7$  for most of their model simulations for mixing efficiency in the Gulf of Aqaba. Elliott and Venayagamoorthy (2011) evaluated four different parameterizations of  $Pr_t$  for stably stratified flows based on gradient Richardson number ( $Ri$ ). The estimates varies between 2–8 when  $Ri = 1$  and between 0.8–3 when  $Ri = 0.25$  in different parameterizations. In this paper, we use different  $Pr_t$  for mixing sensitivity analysis and to examine the impact of mixing-induced heat transfer on the changes in ice formation, thermal stability, and heat storage. Specifically, we configure the model to use MY-2.5 to calculate the  $K_M$  directly, and  $K_H$  is calculated

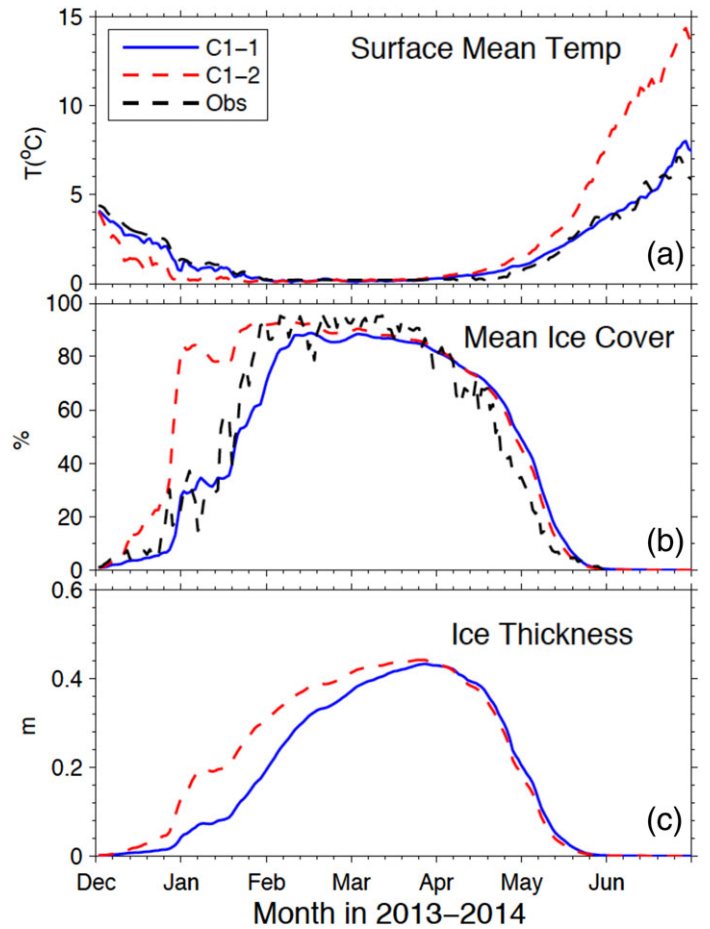


**Fig. 4.** Category 1: The lake-wide mean LST (a), ice cover (b), and ice thickness (c). Blue and red dotted lines are represented for case 1 (C1-1) and case 2 (C1-2), respectively. The Great Lakes Surface Environmental Analysis (GLSEA2) observations (available for LST and ice coverage) are represented by the black dotted line. The GLSEA2 provides lake-wide information on LST and ice coverage, which is produced daily at the NOAA Great Lakes Environmental Research Laboratory (GLERL). The LSTs are derived from NOAA/AVHRR (Advanced Very High Resolution Radiometer) satellite imagery and updated daily with information from the cloud-free portions of the satellite imagery. A smoothing algorithm is applied to the map for days when no imagery available (Schwab et al. 1999). The addition of ice cover concentration was implemented in early 1999, using data provided by the National Ice Center (NIC).

based on a series of prescribed  $Pr_t = 1, 3, 5, 7, 10$  to manipulate vertical thermal mixing. The vertical mixing can be associated with different processes (convection, wind, internal waves, etc.). It should be noted that it was not our aim to examine how different processes influence the change in lake mixing. Instead, our motivation is to understand how the change in vertical lake mixing would impact the change in lake heat content and LST. This approach allows us to manipulate and represent an overall (lumped) change in vertical mixing in the sensitivity analysis without worrying about the causal physical processes. Thus, we could examine the corresponding change in the LST and lake heat content.

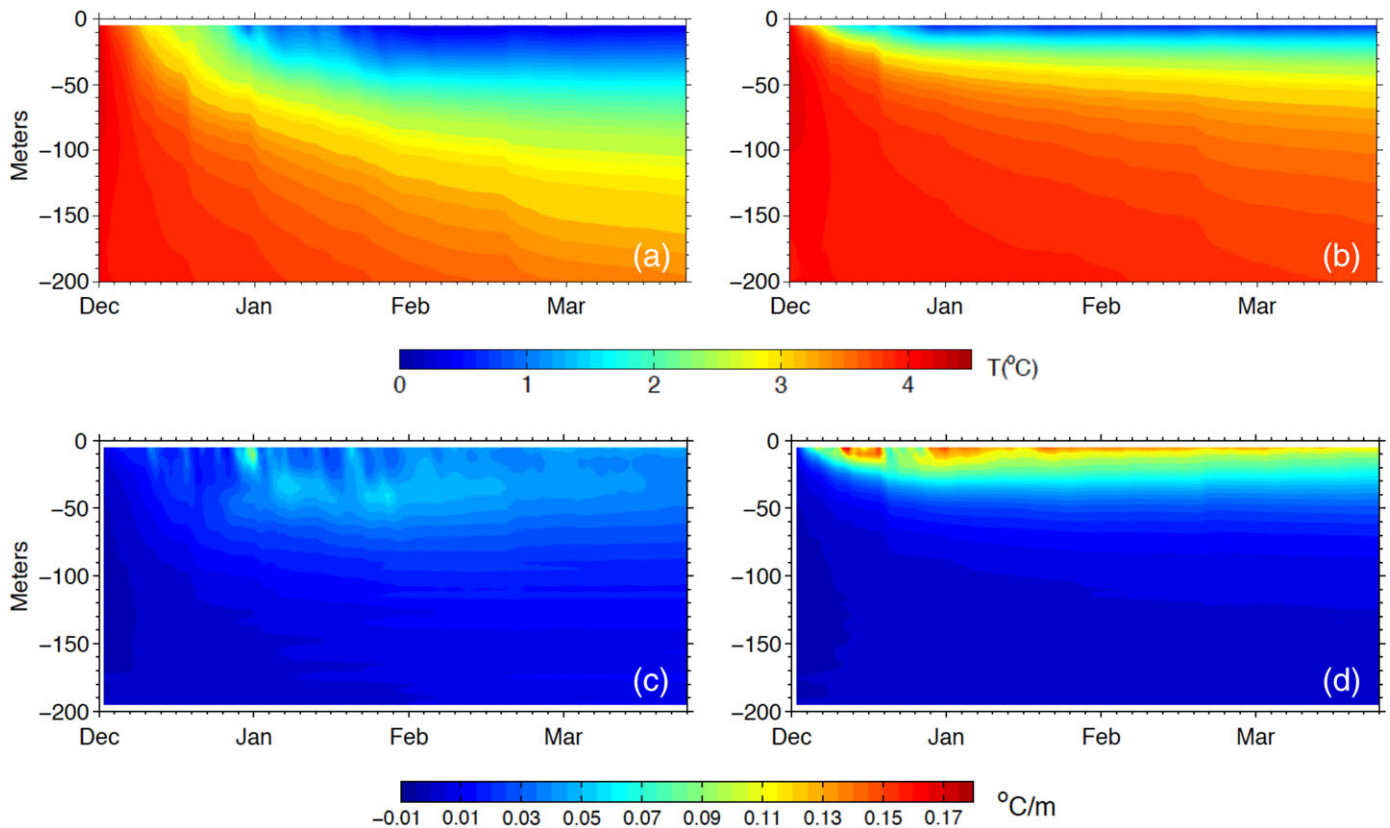


**Fig. 5.** The comparison of case C1-1 (left) and C1-2 (right). Upper panel (**a, b**): time evolution of modeled lake-wide mean temperature profile for lake-wide mean. Lower panel (**c, d**): time evolution of modeled lake-wide mean temperature gradient profile.

### Lake heat content and water density

With a 3D hydrodynamic model, the total lake heat content can be estimated by integrating the heat content from all model cells.

$$H = \sum_{i=1}^n \rho_i C_w V_i T_i$$

where  $H$  is lake heat content,  $V_i$  and  $T_i$  are the volume and water temperature of different element of water in the lake,  $C_w$  is the specific heat of water,  $\rho_i$  is water density of different elements of water. The water density ( $\rho_i$ ) follows the equation of state of Chen and Millero (1977), which uses a polynomial to approximate the equation of state.

### Model configuration and design of the experiments

Xue et al. (2015) examined FVCOM modeling performance in simulating the thermal structure of Lake Superior and analyzed how specific representations of meteorological forcing affect the simulation accuracy of the lake thermal structure. Moreover, taking lake-atmosphere interactions into account, Xue et al. (2017) developed a two-way coupled 3D lake-ice-climate modeling system: Great Lakes–Atmosphere Regional

Model (GLARM). The GLARM has significantly improved the accuracy of the regional climate simulation (Xue et al. 2017). In this study, we adopted the hydrodynamic model component of GLARM as the model performance has been evaluated and validated (see Xue et al. 2017 for model validation). The surface meteorological forcing was obtained from GLARM atmospheric model output.

Despite having experienced warming during the last three decades, the Great Lakes endured the one of most severe winters in 2013–2014 with the lowest temperature and highest ice cover in recent history (NOAA National Climatic Data Center 2014, [Clites et al. 2014]), which has been hypothesized as an indicator of a potential regime shift of the long-term warming trend (Gronewold et al., 2015). Focusing on this extremely cold winter allows us to investigate the four primary research objectives listed in the introduction.

To analyze the relationship between vertical mixing, heat content, ice albedo, and LST, four process-oriented numerical experiments in two categories were designed. In category 1, we analyze the impact of the variation of vertical mixing on the lake conditions of the winter and following spring (cases C1-1 and C1-2). To evaluate how vertical mixing affects heat transfer and thermal structure, the initial conditions and model configuration of those two cases are identical, only the

vertical mixing is changed through the parameterization of  $Pr_t$ . In category 2 (cases C2-1 and C2-2), we analyze the impact of the decreasing ice cover on the accelerated warming of Lake Superior by examining ice albedo feedback and insulation effect. Then, we assess the associated change in heat content and evaluate the role of ice coverage in determining LST for the following spring.

- Case C1-1 serves as a control run. In this case, the  $Pr_t$  is set to the default value of 1, such that the rates of eddy viscosity and eddy diffusivity are equal. The ice albedo is dynamically calculated based on the water temperature and ice thickness using the default ice module configuration in FVCOM (Chen et al. 2006). The model simulation starts from March 1, 2013 with a homogeneous water temperature of 2°C and for a 9-month dynamic adjustment (model spin-up). The model simulation continues until 30 June 2014. Simulation results between December 2013–June 2014 are used for analysis.
- In case C1-2, the model is configured the same as in case C1-1, but the  $Pr_t$  is set to 3, 5, 7, 10, indicating a smaller thermal eddy diffusivity compared to momentum eddy viscosity. This case is restarted from 12/07/2013 using C1-1's restart file to make the two cases comparable for the simulation period of December 2013–June 2014. As the conclusion drawn from the set of experiments are similar (Fig. 3), we use the case with  $Pr_t = 5$  as a representative case for further analysis thereafter as most studies provide estimates of  $Pr_t$  in a range of 1–8.
- In case C2-1, the model configuration is the same as in case C1-1, but ice albedo is prescribed to 0.7 as a constant value, which represents the albedo of bare ice (Zhong et al. 2016). This case is also restarted from December 2013 using case C1-1's restart file.
- In case C2-2, the model configuration is the same as in case C1-1, but the ice albedo is prescribed to a constant number of 0.06 representing the open water albedo value. This case is also restarted from December 2013 using case C1-1's restart file.

A summary of the configuration of these experiments is presented in Table 1.

## Results and discussion

### Category 1: Mixing effect

#### Impact of water mixing on LST and ice

In the experiment category 1 (cases C1-1 and C1-2), the LST decreases from initial 4°C at the beginning of December to ~ 0°C in mid-February during the ice formation phase (Fig. 4a). Compared to the control run (case C1-1), the LST in case C1-2 decreases at a higher rate during the fall and the early winter, the maximum of the mean LST difference between the two cases can reach up to ~ 1°C until the mean LST reaches 0°C in mid-February. The LST starts to increase at

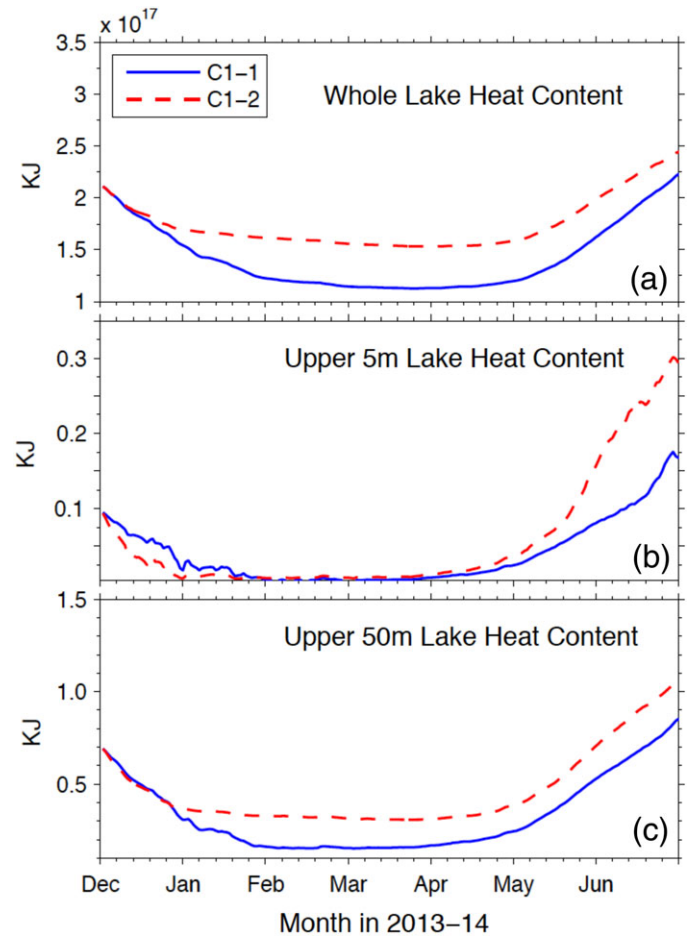


**Fig. 6.** Comparison of heat content in cases C1-1 and C1-2 for the entire lake (a), upper 5 m (b), and upper 50 m (c).

the beginning of April. Similar to the faster decrease in LST in case C1-2, the LST also shows a higher increase rate through April–June with an averaged difference of ~ 2.8°C between case C1-2 and C1-1. The LST in case C1-2 reaches 12.7°C while it is 7.46°C in case C1-1 by the end of June.

Corresponding to the decrease in LST, the ice starts to form in December, and a significant difference in the evolution of ice coverage starts in January. During this time, the ice coverage in case C1-2 increases to 70% while the ice coverage in case C1-1 remains below 30%. The higher ice coverage in case C1-2 persistently increases until mid-February with the highest coverage of 92%. A more linear increase trend of ice coverage is observed in case C1-1 before reaching its peak value of 88% in mid-February. Similarly, the average ice thickness is 0.03–0.13 m greater in case C1-2 than case C1-1 during the ice formation phase in December–February (Fig. 4c). During the ice melting phase between mid-March to early June, there were fewer differences in ice coverage and ice thickness between the two cases, while there was a general overestimation in simulating the mean ice cover in the melting stage for

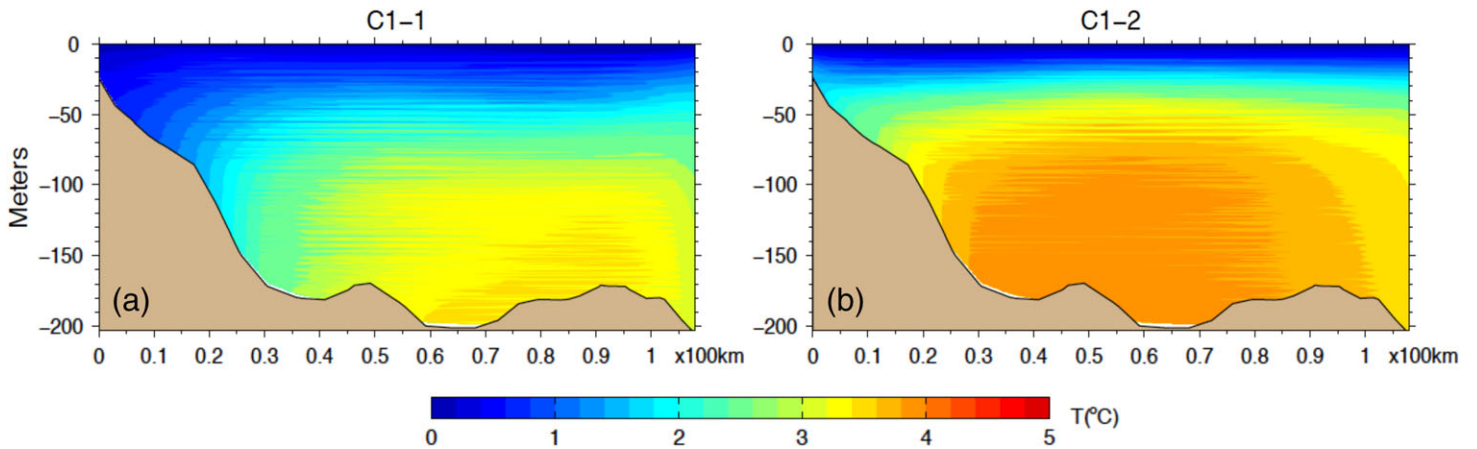


**Fig. 7.** Comparison of cross-sectional temperature in cases C1-1 and C1-2 for the 2014 winter (January–March). See Fig. 2 for the location of the cross-section. X-axis denotes the length of the cross-section, starting from its southeast end.

**Table 2.** Mean value of heat flux components during model simulation period (December 2013–June 2014) in different cases.

Experiment #	SW (W/m <sup>2</sup> )	DLW (W/m <sup>2</sup> )	ULW (W/m <sup>2</sup> )	SHF (W/m <sup>2</sup> )	LHF (W/m <sup>2</sup> )	Net (W/m <sup>2</sup> )
C1-1	88.53	147.72	-177.33	-31.53	-22.59	4.85
C1-2	84.85	133.57	-159.24	-20.93	-17.94	20.30
C2-1	84.61	141.77	-170.28	-31.51	-21.94	2.53
C2-2	94.97	159.91	-191.35	-31.18	-24.63	7.72

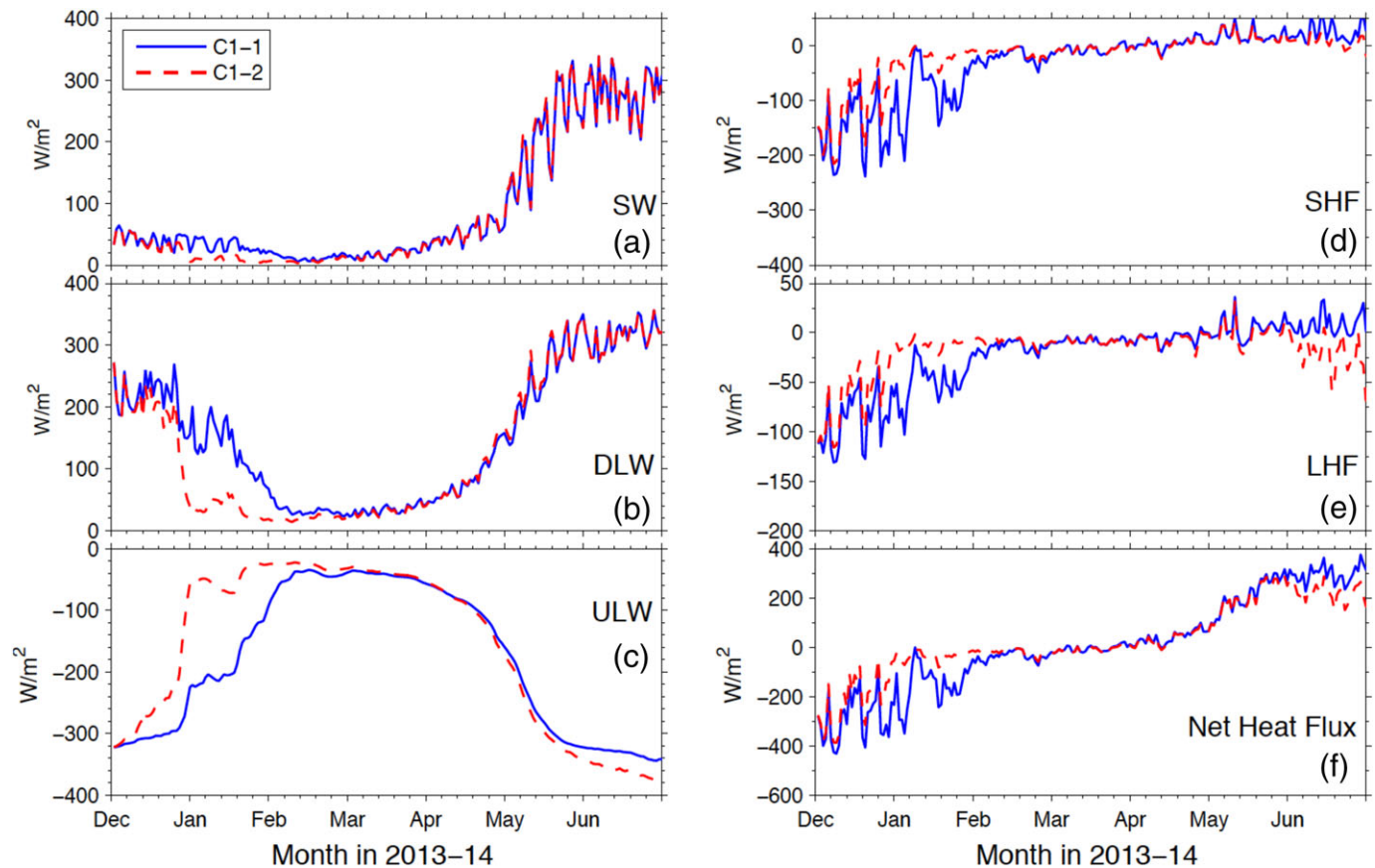


**Fig. 8.** Comparison of surface heat flux radiation in cases C1-1 and C1-2, shortwave radiation (SW) (a), downward longwave radiation (DLW) (b), upper longwave radiation (ULW) (c), sensible heat flux (SHF) (d), latent heat flux (LHF) (e), and net heat flux (f).



both cases. Again, lake-wide ice coverage in case C1-1 generally follows the observed trend in both ice formation and ice melting periods while the ice cover in the ice formation phase is significantly overestimated in case C1-2. Notice a higher rate of ice formation is observed in the case C1-2 during the winter, yet it follows a much faster increase in LSTs in the following 2014 spring as described above. One important outcome from the experiments is that spring and summer LSTs can be considerably influenced by the synchronous effect due to the strength of thermal stratification, in addition to the thermal inertia effects reported by other studies (Piccolroaz et al. 2015; Zhong et al. 2016).

#### Impact of water mixing on heat transfer

During the fall, a decrease in mixing can cause a lower LST which consequently results in higher ice coverage and thickness during the ice formation season. However, a decrease in vertical mixing also causes the dramatic increase in LST in the following spring. This indicates the weakened vertical mixing alters the stratification pattern and serves as an important role in limiting energy transfer between the lake's epilimnion and hypolimnion.

To provide an alternative comparison, Fig. 5a,b display the time evolution of lake-mean temperature profile using temperature results of the depth from 5 m to 200 m as a first-order approximation of the broad lake basin region from December 2013 to March 2014 in cases C1-1 and C1-2. After mixing (overturning) typically occurs in autumn, when the lake is isothermal with the water temperature at  $\sim 4^\circ\text{C}$  throughout the lake in the absence of temperature or density differences, the inverse stratification starts to develop with continuous cooling at the surface layer. The inversely stratified water consistently deepens from less than 50 m in early December to the entire water column at the mid of March for case C1-1. In case C1-2, the inverse stratification becomes stronger and develops a shallower stratified layer; the water stratifies to a depth of 100 m before February and to the maximum depth of 150 m and remains stable throughout March. The time evolution of the lake-mean temperature gradients in cases C1-1 and C1-2 are shown in Fig. 5c,d. Without the direct impact from surface wind due to the extensive ice coverage, strong thermal gradients are shown at the near surface layer. One of the significant differences in the two cases is the much stronger thermal gradient developed in the case C1-2 (Fig. 5c,d), with a gradient of  $> 0.10^\circ\text{C}/\text{m}$  formed near the surface 20 m, while the gradient is much weaker in case C1-1 with a gradient of  $\sim 0.05^\circ\text{C}/\text{m}$  around 40 m deep. Furthermore, the thermal gradient nearly does not exist in case C1-2 below 100 m, showing a very limited transfer of heat in the case of weak mixing.

#### Impact of water mixing on heat content

The total heat budget analysis (Fig. 6) suggests that heat content trends do not necessarily follow trends in LST. Although it is a winter case, the situation is dynamically

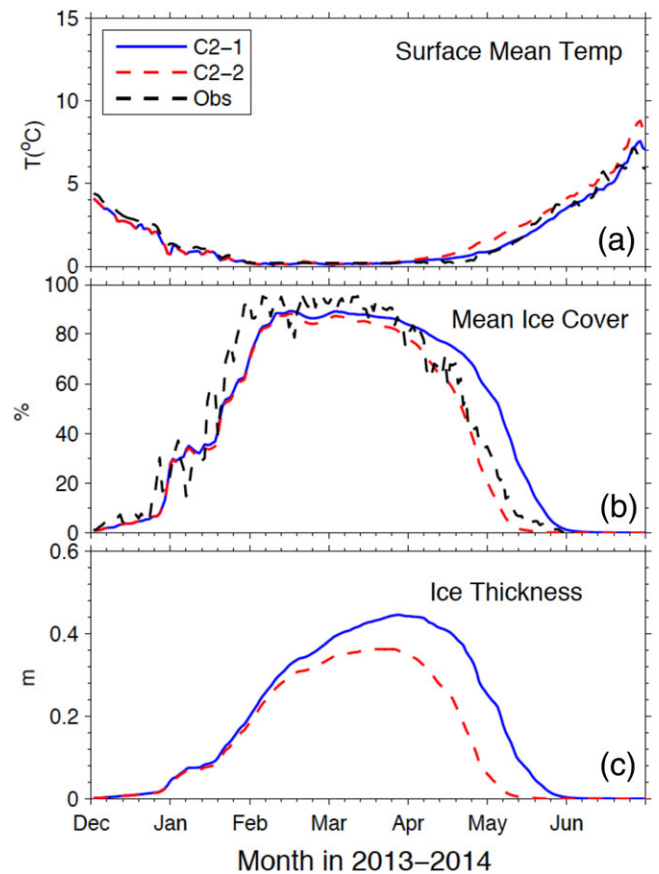


**Fig. 9.** Category 2: The lake-wide mean LST (a), ice cover (b), and ice thickness (c). Blue line and red line represent case C2-1 and case C2-2, respectively. GLSEA2 observations (available for LST and ice coverage) are represented by the black dotted line.

similar to those described by Livingstone and Lotter (1998) and Dokulil (2006). They attribute it to the fact that the downward vertical transport of warm metalimnetic water into the hypolimnion is less efficient in hot summers than in cold summers due to the increased thermal stability (Livingstone and Lotter 1998; George et al. 2007). Similarly, the same phenomenon is also observed in north-central U.S. lakes (Hondzo and Stefan 1993).

Previously, the lake heat content was calculated using the 1D lake conceptual or thermodynamics model for the whole lake (Corley 1992; Gronewold et al., 2015). Still, the spatial temperature varies significantly in Lake Superior due to the steep bathymetry and large surface size, so that the calculation may generate unexpected errors. As described in “Lake heat content and water density” section, we compute heat content (with a reference temperature of  $0^\circ\text{C}$ ) from all model cells to get the lake heat content in each water volume, then integrate all of the water volumes to estimate the heat content of the entire lake.

The water is well mixed during the fall seasons with a net heat loss to the air, therefore both cases show a similar

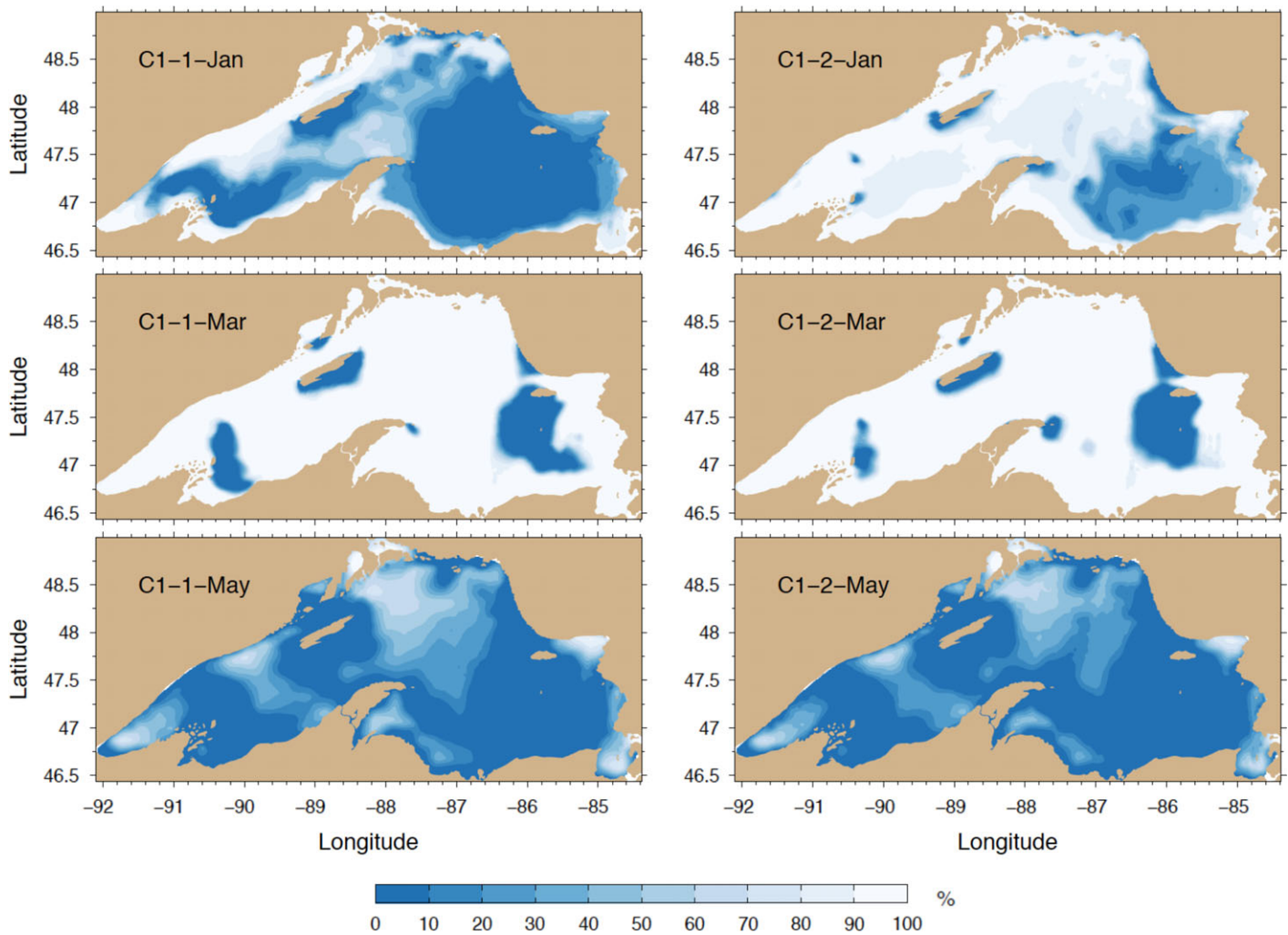


**Fig. 10.** The spatial pattern of mean ice coverage in January, March, and May 2014 for Category 1 case 1 (C1-1) on the left column and case 2 (C1-2) on the right column.

rate of decrease in the total heat content until mid-December before the water inversely stratified (Fig. 6a). The fact that the vertical mixing of case C1-1 is stronger than case C1-2 is apparent during the winter after the water stratification as heat transfer from deeper layer to the surface is much more effective in case C1-1. As a result, surface water is warmer (Figs. 4a, 6b) in case C1-1 after mid-December through January and opposed to ice formation (Fig. 4b,c). Notice although the cold near-surface water forms at a faster pace (quicker decrease in LST) in case C1-2 than in case C1-1 (Figs. 4a, 6b), there is a more significant heat loss in case C1-1 over the entire lake column or even just over the upper 50 m than in case C1-2 (Fig. 6a,c) during the fall and the ice melting period. This suggests that using only LST as an indicator of warming rate could provide misleading information. The trend of decrease in total heat content is weakened in both cases due to the high ice coverage after February, which prevents the heat loss through its

insulation effect. The total heat remains nearly unchanged through March when the lake is largely covered by ice. A reverse trend with similar fashion is observed in the ice melting season. This again suggests that using only LST as a warming indicator can be problematic.

The impact of water mixing on the thermal structure is also evidenced in the cross-sectional winter (January, February, and March) lake temperature (Fig. 7). In case C1-1, the water is well-stratified in the offshore water, with warm water of 3.5°C in the deeper layers. In the shallower region, the vertical mixing process can more easily affect the entire water column, and the stratification is relatively weak. A similar pattern is shown in case C1-2 as well, but the deeper water is warmer by ~ 0.5°C and surface layer is colder, which results in a much sharper thermal gradient at ~ 20–40 m. This is consistent with the time evolution of the temperature profile (Fig. 5). The warmer water exists in the deep layer in case C1-2 with a thin layer of cold water at the surface while the more substantial

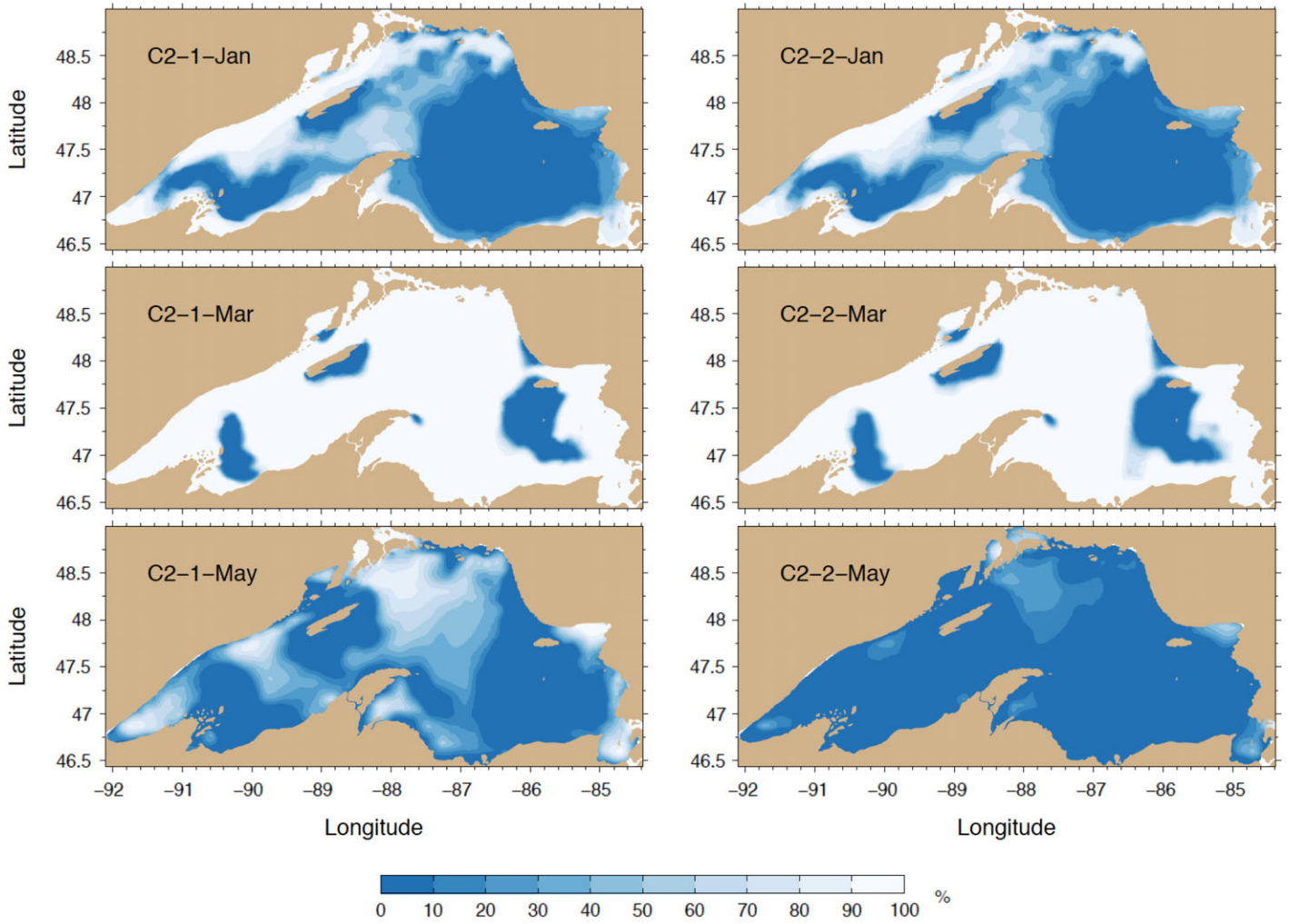


**Fig. 11.** The spatial pattern of mean ice coverage in January, March, and May 2014 for Category 2 case1 (C2-1) on the left column and case2 (C2-2) on the right column.

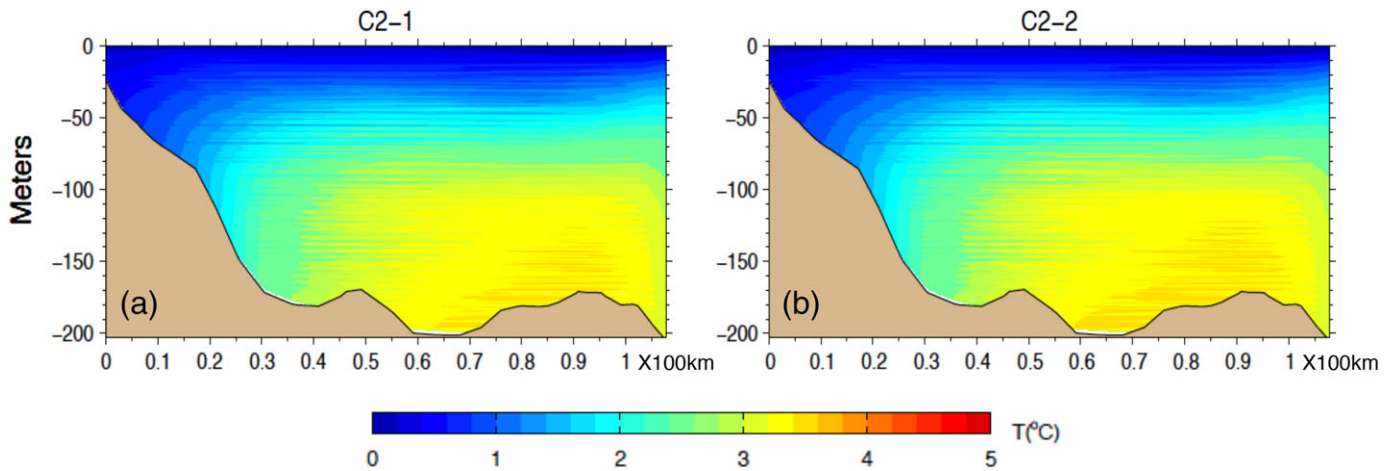


**Fig. 12.** Comparison of cross-sectional temperature in cases C2-1 and C2-2 for the 2014 winter (January–March). See Fig. 2 for the location of the cross-section. X-axis denotes the length of the cross-section, starting from its southeast end.



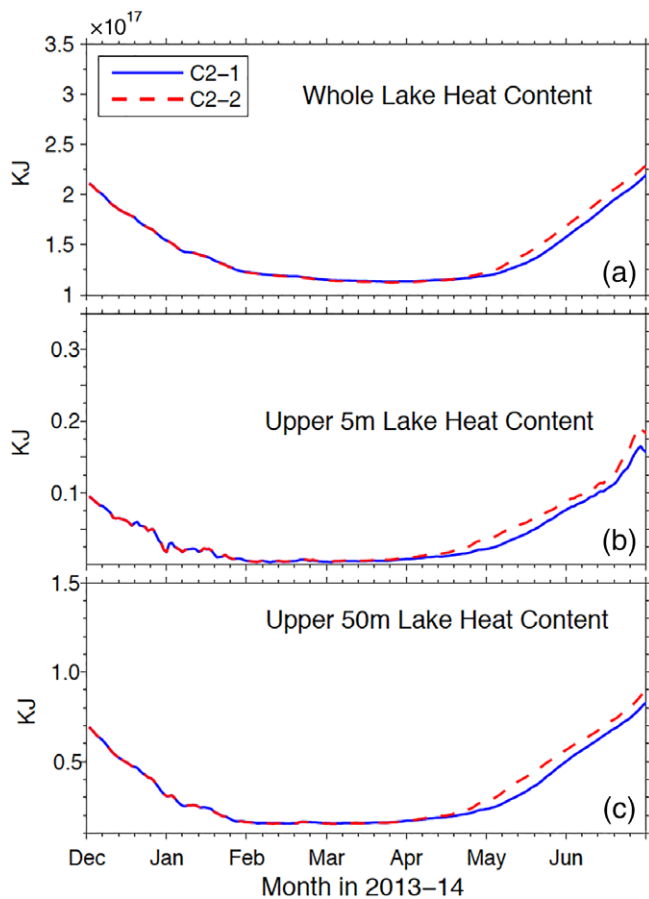


**Fig. 13.** Comparison of heat content in cases C2-1 and C2-2 for the entire lake (a), upper 5 m (b), and upper 50 m (c).

mixing in the case C1-1 results in a colder water in the deep layer. This is due to the more efficient heat transfer to the upper layer and eventual loss to the atmosphere. Both analyses support the conclusion from the comparison of heat content in the two cases in Fig. 6.

#### Impact of water mixing on surface heat fluxes

The analysis of surface heat flux shows a connection between the lake surface condition and the atmospheric condition. The net heat flux,  $H$ , is computed as:

$$H = H_{sw} + H_{LW} + H_{SHF} + H_{LHF}$$

where  $H_{sw}$  is the net shortwave radiation (SW),  $H_{LW}$  is the net long wave radiative flux,  $H_{SHF}$  is the sensible heat flux (SHF), and  $H_{LHF}$  is the latent heat flux (LHF). The mean value of the heat flux components during the entire model simulation period (December 2013–June 2014) in different cases is summarized in Table 2. The net heat flux exhibits a seasonal signal (Fig. 8). The net flux is negative (heat loss from the lake) from December to February 2014, close to zero during the high ice coverage and low solar radiation (February–April), and are

positive (heat absorbed by the lake) during the spring. Shortwave radiation flux, net long wave radiation, sensible heat flux, and latent heat flux all contribute to the seasonal trend of net heat flux (Fig. 8), indicating strong feedbacks occur in the coupled system across the atmosphere–water interface, which regulate lake temperature and heat fluxes (Xue et al. 2017).

During the ice formation period (December 2013–February 2014), the upward longwave radiation (ULW) (Fig. 8c) with a mean value of  $-146.85 \text{ W/m}^2$  (negative value indicates a loss of heat from the lake) in case C1-1 and  $-106.35 \text{ W/m}^2$  in case C1-2, sensible heat flux (SHF) (Fig. 8d) with a mean value of  $-68.47 \text{ W/m}^2$  (C1-1) and  $-46.85 \text{ W/m}^2$  (C1-2) and latent heat flux (LHF) (Fig. 8e) with a mean value of  $-41.61 \text{ W/m}^2$  (C1-1) and  $-28.52 \text{ W/m}^2$  (C1-2) are all important to surface heat loss. The differences in the surface heat fluxes are in response to the noticeable difference of ice coverage in ice formation period in the two cases. The ice coverage in case C1-2 is nearly 30% higher than case C1-1, the ice coverage prevents the heat loss from water to atmosphere (ULW, SHF and LHF (Fig. 8c,d, e), resulting in a difference during this period in ULW of  $\sim -40.5 \text{ W/m}^2$ , SHF of  $\sim -21.6 \text{ W/m}^2$ , and LHF of  $-13.1 \text{ W/m}^2$  between cases C1-1 and C1-2 (C1-1 minus C1-2) and the heat absorption (SW + DLW (Fig. 8a,b) of  $35.8 \text{ W/m}^2$  (C1-1 minus C1-2) from atmosphere to water. As a result, the net heat flux to the atmosphere in case C1-2 is lower than that in case C1-1 ( $-39.4 \text{ W/m}^2$ ) in the ice formation period. This reinforces more heat losses in case C1-1 with stronger mixing, resulting in lower ice coverage and lower total heat content.

In the spring (April–June 2014), the shortwave radiation (SW) (Fig. 8a) ( $166.1 \text{ W/m}^2$  in C1-1 and  $167.4 \text{ W/m}^2$  in C1-2, [positive value indicates heat gain to the lake]) increases significantly, however, SW are nearly identical in value in cases C1-1 and C-2. The major difference in the net surface heat flux arises from the loss of heat through SHF (Fig. 8d) with a difference of  $3.1 \text{ W/m}^2$  (C1-1 minus C1-2), LHF (Fig. 8e) with a difference of  $6.1 \text{ W/m}^2$  (C1-1 minus C1-2), and ULW with a difference of  $9.6 \text{ W/m}^2$  due to a more substantial air–sea temperature difference in case C1-2, as revealed by the LSTs comparison. Thus, the lake receives less heat flux in case C1-2 than case C1-1 by  $17.23 \text{ W/m}^2$ .

#### Category 2: Ice albedo feedback

Ice conditions due to climate variation impact thermal energy and biogeochemical processes. However, it is still unclear how does the ice albedo affect the surface heat flux, ice mass, and thermal structure in Lake Superior. The experiments in category 2 (cases C2-1 and C2-2) are designed to examine the impact of ice albedo by setting the ice albedo as 0.7 for bare ice (case C2-1) and as 0.06 for the albedo of open water surface (case C2-2). These are two extreme cases in comparison with the control run (C1-1), in which albedo is dynamically calculated.

Results show that the ice albedo affects LST primarily, but not significantly, during the ice melting phase. The mean LST



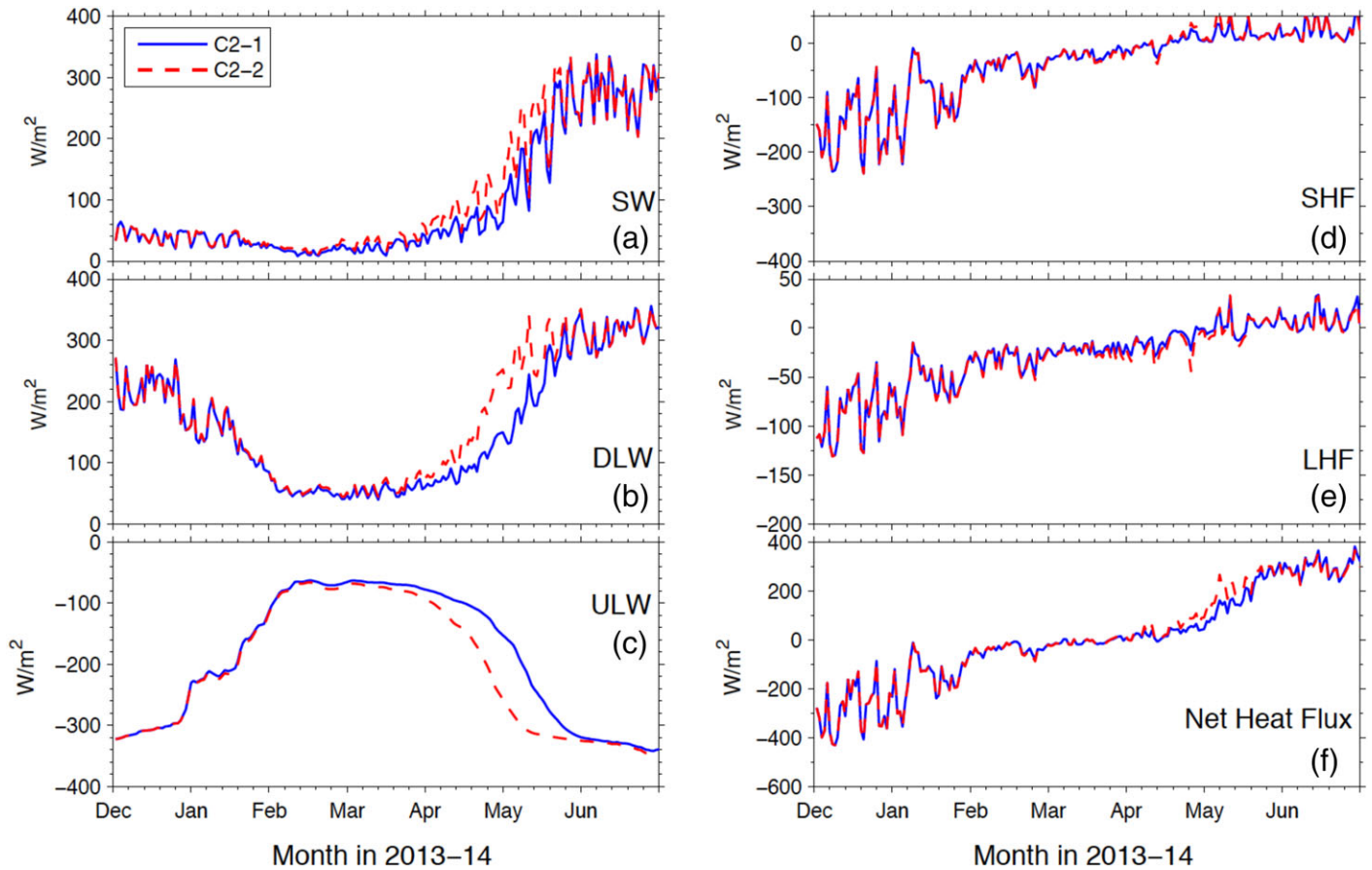


**Fig. 14.** Comparison of surface heat flux radiation in cases C2-1 and C2-2, shortwave radiation (SW) (a), downward longwave radiation (DLW) (b), upper longwave radiation (ULW) (c), sensible heat flux (SHF) (d), latent heat flux (LHF) (e), and net heat flux (f).

(Fig. 9a) in the two cases shows a nearly identical evolution from the initial  $4^{\circ}\text{C}$  at the beginning of December to  $\sim 0^{\circ}\text{C}$  at the mid of March during the ice formation period. The LST evolves differently beginning in April when LSTs are warmer in case C2-2 than C2-1 by an average of only  $0.25^{\circ}\text{C}$  until June. In comparison to experiments in category 1, this suggests the impact of the water mixing effect can potentially be more significant than the ice albedo effect on LST variability during a cold year.

In the ice formation period, the ice cover and thickness show little difference between the two cases (Fig. 9b,c). During maximal ice cover (mid-February–late March), the ice concentration remains the same but ice thickness shows increasing difference. In the ice melting phase, both ice cover and thickness show considerable differences. The ice is much thicker by an average of  $0.2\text{ m}$  in case C2-1 than C2-2. Furthermore, the ice coverage in case C2-1 lasts nearly 5 months (January–early June) while no ice exists in mid-May in case C2-2. This is different from the category 1 experiment, where the change in water mixing primarily affected the ice coverage during the ice formation period and has little impact on the ice melting period. Such a difference can also be viewed

from the heterogeneity of spatial distribution of ice coverage (Mason et al. 2016) in the two categories, as presented in Figs. 10, 11. In category 1, at the beginning of the ice formation period, more ice forms in the western and the central basins and southern coastal region in case C1-2 compared with case C1-1 in January 2014, until the lake is nearly fully covered by ice in March in both cases. During the ice melting season, ice melts at a similar rate until the end of May in both cases. In category 2, there is no significant difference between ice coverage in the two cases from January to March during the ice formation period. In May, the ice coverage in case C2-1 is still noticeable, while the ice coverage in case C2-2 is  $< 10\%$ .

In contrast to category 1, there is no significant difference in water stratification profiles in the simulation cases in category 2 (Fig. 12). In fact, the stratification pattern from both category 2 cases during the winter time is very similar to case C1-1. This indicates the different parameterization (e.g., constant albedo of bare ice, dynamically calculated albedo, and water albedo) of ice albedo provides less impact on the lake thermal stratification in the winter, regardless of its noticeable effects on ice melting near the surface layer.

However, the albedo effect is not strictly limited to the surface layer (Fig. 13c). The fact that the difference in lake heat content at the ice melting stage is consistent with model behavior in ice coverage and thickness and reflects the impact of the albedo effect on surface heat flux, subsurface temperature, and, therefore, heat content (Fig. 13).

While category 1 (cases C1-1 and C1-2) shows that mixing primarily affects the surface heat fluxes during ice formation, the results in category 2 (cases C2-1 and C2-2) reveals that the ice albedo effects on surface heat flux primarily occur during the ice melting period (April–June 2014) as displayed in Fig. 14. As the ice albedo is parameterized from 0.7 to 0.06, in the ice melting period, the mean value of SW (Fig. 14a) increases by  $22 \text{ W/m}^2$  and the net longwave radiation (DLW + ULW, Fig. 14b,c) decreases by  $5 \text{ W/m}^2$ . The mean value of SHF and LHF (Fig. 14d,e) increases by  $2.6 \text{ W/m}^2$  and decreases by  $4.4 \text{ W/m}^2$ , respectively. This results in an increase in the net heat flux (Fig. 14f) by  $\sim 15 \text{ W/m}^2$ . The results from this case illustrate the effects of ice albedo on lake surface heat flux in an extremely cold year during which the total incoming solar radiation is typically weak.

## Conclusion

Using the numerical model to manipulate and analyze the lake lumped vertical mixing and ice albedo allows us to better understand the processes controlling thermal stratification and heat budget in a large, deep lake and their impacts on potential lake response to climate change. Our analysis suggests that even though the heat content is calculated by temperature, the tendency of change in heat content does not necessarily follow the trend of LST, which is also supported by other observation-based studies for north-central U.S. lakes (Hondzo and Stefan 1993). This is because stronger mixing may slow down the decrease in LST in the cooling season due to more effective heat supply from deep water to the surface layer, hence reduce the surface ice formation. As a result, it also causes more effective heat loss to the atmosphere, thus reducing the total heat content of the lake. Similarly, in the warming season, stronger mixing can slow down the increase in LST by transferring more heat into a deeper layer. Therefore, one may observe lower LST but high lake heat content in the spring. As the heat content is much more ecologically significant, the results suggest that the lake heat content should be a more appropriate indicator to infer climate-induced lake warming.

The presence of ice in the Great Lakes further complicates how mixing affects the change in the lake thermal structure and heat content. During the ice formation period, the stronger (weaker) mixing slow down (speed up) the cooling of LST, which causes the later (earlier) freezing of the lake. Our results show that water mixing primarily affects ice coverage during the ice formation period and has little influence on the ice cover during the ice melting period. This suggests that the

energy for ice melting is primarily driven by solar radiation rather than the water, which is also evidenced by the surface heat flux budget.

By comparing model behavior with and without ice-albedo effect, it shows that the ice albedo in the 2013–2014 winter does not play a major role in determining the late spring surface warming. Moreover, additional category 2 experiments (not shown) were run to investigate the milder winter conditions associated with the 1997–1998 El Niño event (Kumar et al., 2001). Results reveal that the change in surface albedo, during the winter of 1997–1998, plays a minor role in LST variability, similar to Zhong et al. (2016). These results suggest the ice albedo effect does not have a significant impact in Lake Superior in either the cold winter (2013–2014) or the warm winter (1997–1998). This is because Lake Superior is only covered by seasonal ice and is always ice-free during the summertime. The ice albedo effect is limited in the winter and spring, therefore is insignificant due to low incident solar irradiance (e.g., cold winter) and/or low ice coverage (e.g., warm winter).

This situation is different from that in the Arctic Ocean (AO). The AO is characterized by two major ice classes (perennial and seasonal ice), and the ice albedo feedback can create major effects throughout the summer. Before the onset of melt in spring, both seasonal and multiyear ice are covered by snow, and very little solar energy is absorbed by the Arctic ice-ocean system (Perovich & Polashenski, 2012). The albedo and absorbed solar energy begin to diverge in late May throughout the summer when the incident solar energy is high, and the change in albedo and ice melt have significant impacts on total solar energy absorbed in the ice-ocean system (Perovich et al. 2007a,b). Furthermore, an ongoing shift of ice cover from perennial ice to seasonal ice (Nghiem et al. 2007; Serreze et al. 2007) and lengthening of the summer ice melting season (Markus et al. 2009) allows for more solar energy to be absorbed in the ice-ocean system during the summer. This leads to more efficient seasonal ice melt and further ice reduction through the ice albedo feedback (Perovich & Polashenski, 2012).

This study provides an improved understanding of the complex physical mechanisms that control the variation of lake physical characteristics in response to a changing climate. Our results indicate that climate change will not only affect the air-lake energy exchange but will further alter lake internal dynamics, hence the lake's response to ongoing climate change may vary with time. The complexity of the dynamics in large, deep lakes makes it much more challenging and less reliable to use a traditional regional climate model (RCM) to predict climate variability for the Great Lakes region. The most suitable approach is to take a regional earth-system modeling approach by applying a RCM two-way coupled with a 3D hydrodynamic model across the Great Lakes region (Xue et al. 2017).

It should be noted that we used a previously validated model configuration for this study and it was not our intent to put major efforts for further improvement of the simulation

results of the Lake Superior winter condition. Instead, using these process-oriented numerical experiments, we demonstrate that model parameterizations can be an effective way of detecting a subtle pattern of change, and, as a result, quantify the sensitivity of lake response to a changing climate. Furthermore, these results also suggest that extra attention must be paid when calibrating and tuning models to decipher the impacts of climate change and the hydrodynamic response of the lake in future modeling studies. For example, a change in mixing parameterization can effectively alter the ice formation and LST, yet it may result in unintended larger bias in the total heat content. Overall, more effort should be given toward model development and parameterization for large lake systems, such as the Great Lakes, with comprehensive phenological and dynamic validation.

## References

- Adrian, R., N. Walz, T. Hintze, S. Hoeg, and R. Rusche. 1999. Effects of ice duration on plankton succession during spring in a shallow polymictic lake. *Freshw. Biol.* **41**: 621–634. doi:10.1046/j.1365-2427.1999.00411.x
- Adrian, R., and others. 2009. Lakes as sentinels of climate change. *Limnol. Oceanogr.* **54**: 2283–2297, DOI: 10.4319/lo.2009.54.6\_part\_2.2283
- Anderson, E. J., and D. J. Schwab. 2013. Predicting the oscillating bi-directional exchange flow in the Straits of Mackinac. *J. Great Lakes Res.* **39**: 663–671. doi:10.1016/j.jglr.2013.09.001
- Arvola L. et al. (2009) The Impact of the Changing Climate on the Thermal Characteristics of Lakes. In: George G. (eds) The Impact of Climate Change on European Lakes. Aquatic Ecology Series, vol 4. Springer, Dordrecht. DOI:10.1007/978-90-481-2945-4\_6
- Austin, J. A., and S. M. Colman. 2007. Lake Superior summer water temperatures are increasing more rapidly than regional air temperatures: A positive ice-albedo feedback. *Geophys. Res. Lett.* **34**: L06604. doi:10.1029/2006GL029021
- Austin, J., and S. Colman. 2008. A century of temperature variability in Lake Superior. *Limnol. Oceanogr.* **53**: 2724–2730. doi:10.4319/lo.2008.53.6.2724
- Beardsley, R. C., C. Chen, and Q. Xu. 2013. Coastal flooding in Scituate (MA): A FVCOM study of the 27 December 2010 nor'easter. *J. Geophys. Res. Oceans* **118**: 6030–6045. doi:10.1002/2013JC008862
- Bennington, V., G. A. McKinley, N. Kimura, and C. H. Wu. 2010. General circulation of Lake Superior: Mean, variability, and trends from 1979 to 2006. *J. Geophys. Res. Oceans* **115**: C12015. doi:10.1029/2010JC006261
- Burnett, A. W., M. E. Kirby, H. T. Mullins, and W. P. Patterson. 2003. Increasing Great Lake–effect snowfall during the twentieth century: A regional response to global warming? *J. Clim.* **16**: 3535–3542. doi:10.1175/1520-0442(2003)016<3535:IGLSDT>2.0.CO;2
- Butcher, J. B., D. Nover, T. E. Johnson, and C. M. Clark. 2015. Sensitivity of lake thermal and mixing dynamics to climate change. *Clim. Change* **129**: 295–305. doi:10.1007/s10584-015-1326-1
- Chen, C., and F. J. Millero. 1977. The use and misuse of pure water PVT properties for lake waters. *Nature* **266**: 707–708. doi:10.1038/266707a0
- Chen, C., R. C. Beardsley, and G. Cowles. 2006. An unstructured grid, finite-volume coastal ocean model (FVCOM) system. *Oceanography* **19**: 78–89. doi:10.5670/oceanog.2006.92
- Clites, A. H., J. Wang, K. B. Campbell, A. D. Gronewold, R. A. Assel, X. Bai, and G. A. Leshkevich. 2014. Cold water and high ice cover on Great Lakes in spring 2014. *Eos Trans. Am. Geophys. Union* **95**: 305–306. doi:10.1002/2014EO340001
- Croley II, T. E. 1992. Long-term heat storage in the Great Lakes. *Water Resour. Res.* **28**: 69–81. doi:10.1029/91WR02500
- Coats, R., J. Perez-Losada, G. Schladow, R. Richards, and C. Goldman. 2006. The warming of Lake Tahoe. *Clim. Change* **76**: 121–148. doi:10.1007/s10584-005-9006-1
- Collingsworth, P. D., and others. 2017. Climate change as a long-term stressor for the fisheries of the Laurentian Great Lakes of North America. *Rev. Fish Biol. Fish.* **27**: 363–391, DOI: 10.1007/s11160-017-9480-3
- Desai, A. R., J. A. Austin, V. Bennington, and G. A. McKinley. 2009. Stronger winds over a large lake in response to weakening air-to-lake temperature gradient. *Nat. Geosci.* **2**: 855–858. doi:10.1038/ngeo693
- Dobiesz, N. E., and N. P. Lester. 2009. Changes in mid-summer water temperature and clarity across the Great Lakes between 1968 and 2002. *J. Great Lakes Res.* **35**: 371–384. doi:10.1016/j.jglr.2009.05.002
- Dokulil, M. T., and others. 2006. Twenty years of spatially coherent deepwater warming in lakes across Europe related to the North Atlantic oscillation. *Limnol. Oceanogr.* **51**: 2787–2793, DOI: 10.4319/lo.2006.51.6.2787
- Drinkwater, K. F., and others. 2003. The response of marine ecosystems to climate variability associated with the North Atlantic oscillation. Wiley Online Library.
- Dunckley, J. F., J. R. Koseff, J. V. Steinbuck, S. G. Monismith, and A. Genin. 2012. Comparison of mixing efficiency and vertical diffusivity models from temperature microstructure. *J. Geophys. Res. Oceans* **117**: C10008. doi:10.1029/2012JC007967
- Elliott, Z. A., and S. K. Venayagamoorthy. 2011. Evaluation of turbulent Prandtl (Schmidt) number parameterizations for stably stratified environmental flows. *Dyn. Atmos. Oceans* **51**: 137–150. doi:10.1016/j.dynatmoce.2011.02.003
- Fink, G., M. Schmid, B. Wahl, T. Wolf, and A. Wüest. 2014. Heat flux modifications related to climate-induced warming of large European lakes. *Water Resour. Res.* **50**: 2072–2085. doi:10.1002/2013WR014448
- Fujisaki-Manome, A., L. E. Fitzpatrick, A. D. Gronewold, E. J. Anderson, B. M. Lofgren, C. Spence, J. Chen, C. Shao,

- D. M. Wright, and C. Xiao. 2017. Turbulent heat fluxes during an extreme lake-effect snow event. *J. Hydrometeorol.* **18**: 3145–3163. doi:[10.1175/JHM-D-17-0062.1](https://doi.org/10.1175/JHM-D-17-0062.1)
- George, G., M. Hurley, and D. Hewitt. 2007. The impact of climate change on the physical characteristics of the larger lakes in the English Lake District. *Freshw. Biol.* **52**: 1647–1666. doi:[10.1111/j.1365-2427.2007.01773.x](https://doi.org/10.1111/j.1365-2427.2007.01773.x)
- Gerten, D., and R. Adrian. 2000. Climate-driven changes in spring plankton dynamics and the sensitivity of shallow polymictic lakes to the North Atlantic oscillation. *Limnol. Oceanogr.* **45**: 1058–1066. doi:[10.4319/lo.2000.45.5.1058](https://doi.org/10.4319/lo.2000.45.5.1058)
- Goodman, L., and E. R. Levine. 2003. Use of Turbulent Kinetic Energy and Scalar Variance Budgets to Obtain Directly Eddy Viscosity and Diffusivity from AUV Turbulence Measurements. Retrieved from <https://www.semanticscholar.org/paper/Use-of-Turbulent-Kinetic-Energy-and-Scalar-Variance-Goodman-Levine/3aaa3e6a586d661a4a6d0550d116c59de3d1841d>
- Gorham, E. 1964. Morphometric control of annual heat budgets in temperate lakes. *Limnol. Oceanogr.* **9**: 525–529. doi:[10.4319/lo.1964.9.4.0525](https://doi.org/10.4319/lo.1964.9.4.0525)
- Gronewold, A. D., E. J. Anderson, B. Lofgren, P. D. Blanken, J. Wang, J. Smith, T. Hunter, G. Lang, C. A. Stow, D. Beletsky, and J. Bratton (2015), Impacts of extreme 2013–2014 winter conditions on Lake Michigan’s fall heat content, surface temperature, and evaporation. *Geophys. Res. Lett.*, **42**, 3364–3370. doi:[10.1002/2015GL063799](https://doi.org/10.1002/2015GL063799).
- Hondzo, M., and H. G. Stefan. 1993. Regional water temperature characteristics of lakes subjected to climate change. *Clim. Change* **24**: 187–211. doi:[10.1007/BF01091829](https://doi.org/10.1007/BF01091829)
- Kumar, A., W. Q. Wang, M. P. Hoerling, A. Leetmaa, and M. Ji. 2001. The sustained North American warming of 1997 and 1998. *J. Clim.* **14**: 345–353. doi:[10.1175/1520-0442\(2001\)014<0345:TSNAWO>2.0.CO;2](https://doi.org/10.1175/1520-0442(2001)014<0345:TSNAWO>2.0.CO;2)
- Lenters, J. D., J. B. Anderson, P. Blanken, C. Spence, and A. E. Suyker. 2013. Assessing the impacts of climate variability and change on Great Lakes evaporation. *In* D. Brown, D. Bidwell, and L. Briley [eds.], 2011 Project Reports.
- Livingstone, D. M. 2003. Impact of secular climate change on the thermal structure of a large temperate central European Lake. *Clim. Change* **57**: 205–225. doi:[10.1023/A:1022119503144](https://doi.org/10.1023/A:1022119503144)
- Livingstone, D. M., and A. F. Lotter. 1998. The relationship between air and water temperatures in lakes of the Swiss Plateau: A case study with palaeolimnological implications. *J. Paleolimnol.* **19**: 181–198. doi:[10.1023/A:1007904817619](https://doi.org/10.1023/A:1007904817619)
- Lynch, A., W. Taylor, and K. Smith. 2010. The influence of changing climate on the ecology and management of selected Laurentian Great Lakes fisheries. *J. Fish Biol.* **77**: 1764–1782. doi:[10.1111/j.1095-8649.2010.02759.x](https://doi.org/10.1111/j.1095-8649.2010.02759.x)
- Markus, T., J. C. Stroeve, and J. Miller. 2009. Recent changes in Arctic Sea ice melt onset, freezeup, and melt season length. *J. Geophys. Res.* **114**: C12024. doi:[10.1029/2009JC005436](https://doi.org/10.1029/2009JC005436)
- Mason, L. A., C. M. Riseng, A. D. Gronewold, E. S. Rutherford, J. Wang, A. Clites, S. D. Smith, and P. B. McIntyre. 2016. Fine-scale spatial variation in ice cover and surface temperature trends across the surface of the Laurentian Great Lakes. *Clim. Change* **138**: 71–83. doi:[10.1007/s10584-016-1721-2](https://doi.org/10.1007/s10584-016-1721-2)
- Mazumder, A., and W. D. Taylor. 1994. Thermal structure of lakes varying in size and water clarity. *Limnol. Oceanogr.* **39**: 968–976. doi:[10.4319/lo.1994.39.4.0968](https://doi.org/10.4319/lo.1994.39.4.0968)
- McCormick, M. J., and G. L. Fahnenstiel. 1999. Recent climatic trends in nearshore water temperatures in the St. Lawrence Great Lakes. *Limnol. Oceanogr.* **44**: 530–540. doi:[10.4319/lo.1999.44.3.0530](https://doi.org/10.4319/lo.1999.44.3.0530)
- Mellor, G. L., and T. Yamada. 1982. Development of a turbulence closure model for geophysical fluid problems. *Rev. Geophys.* **20**: 851–875. doi:[10.1029/RG020i004p00851](https://doi.org/10.1029/RG020i004p00851)
- Muench, R., L. Padman, A. Gordon, and A. Orsi. 2009. A dense water outflow from the Ross Sea, Antarctica: Mixing and the contribution of tides. *J. Mar. Syst.* **77**: 369–387. doi:[10.1016/j.jmarsys.2008.11.003](https://doi.org/10.1016/j.jmarsys.2008.11.003)
- Nghiem, S. V., I. G. Rigor, D. K. Perovich, P. Clemente-Colón, J. W. Weatherly, and G. Neumann. 2007. Rapid reduction of Arctic perennial sea ice. *Geophys. Res. Lett.* **34**: L19504. doi:[10.1029/2007GL031138](https://doi.org/10.1029/2007GL031138)
- Noh, Y., Y. J. Kang, T. Matsuura, and S. Iizuka. 2005. Effect of the Prandtl number in the parameterization of vertical mixing in an OGCM of the tropical Pacific. *Geophys. Res. Lett.* **32**: L23609. doi:[10.1029/2005GL024540](https://doi.org/10.1029/2005GL024540)
- O’Reilly, C. M., S. R. Alin, P. Plisnier, A. S. Cohen, and B. A. McKee. 2003. Climate change decreases aquatic ecosystem productivity of Lake Tanganyika, Africa. *Nature* **424**: 766–768. doi:[10.1038/nature01833](https://doi.org/10.1038/nature01833)
- O’Reilly, C. M., S. Sharma, D. K. Gray, S. E. Hampton, J. S. Read, R. J. Rowley, P. Schneider, J. D. Lenters, P. B. McIntyre, B. M. Kraemer, et al. 2015. Rapid and highly variable warming of lake surface waters around the globe. *Geophys. Res. Lett.* **42**: 10,773–10,781. doi:[10.1002/2015GL066235](https://doi.org/10.1002/2015GL066235)
- Perovich, D. K., T. C. Grenfell, B. Light, and P. Hobbs. 2002. Seasonal evolution of the albedo of multiyear Arctic Sea ice. *J. Geophys. Res. Oceans* **107**: 8044. doi:[10.1029/2000JC000438](https://doi.org/10.1029/2000JC000438)
- Perovich, D. K., B. Light, H. Eicken, K. F. Jones, K. Runciman, and S. V. Nghiem. 2007a. Increasing solar heating of the Arctic Ocean and adjacent seas, 1979–2005: Attribution and role in the ice-albedo feedback. *Geophys. Res. Lett.* **34**: L19505. doi:[10.1029/2007GL031480](https://doi.org/10.1029/2007GL031480)
- Perovich, D. K., S. V. Nghiem, T. Markus, and A. Schweiger. 2007b. Seasonal evolution and interannual variability of the local solar energy absorbed by the Arctic Sea ice–ocean system. *J. Geophys. Res. Oceans* **112**: C03005. doi:[10.1029/2006JC003558](https://doi.org/10.1029/2006JC003558)
- Perovich, D. K., and C. Polashenski. 2012. Albedo evolution of seasonal Arctic Sea ice. *Geophys. Res. Lett.* **39**: L08501. doi:[10.1029/2012GL051432](https://doi.org/10.1029/2012GL051432)
- Piccolroaz, S., M. Toffolon, and B. Majone. 2015. The role of stratification on lakes’ thermal response: The case of Lake



- Superior. *Water Resour. Res.* **51**: 7878–7894. doi:[10.1002/2014WR016555](https://doi.org/10.1002/2014WR016555)
- Robertson, D. M., and R. A. Ragotzkie. 1990. Changes in the thermal structure of moderate to large sized lakes in response to changes in air temperature. *Aquat. Sci.* **52**: 360–380. doi:[10.1007/BF00879763](https://doi.org/10.1007/BF00879763)
- Safaie, A., E. Litchman, and M. S. Phanikumar. 2017. Evaluating the role of groundwater in circulation and thermal structure within a deep inland lake. *Adv. Water Resour.* **108**: 310–327. doi:[10.1016/j.advwatres.2017.08.002](https://doi.org/10.1016/j.advwatres.2017.08.002)
- Scheffer, M., D. Straile, E. H. van Nes, and H. Hoser. 2001. Climatic warming causes regime shifts in lake food webs. *Limnol. Oceanogr.* **46**: 1780–1783. doi:[10.4319/lo.2001.46.7.1780](https://doi.org/10.4319/lo.2001.46.7.1780)
- Schneider, P., S. J. Hook, R. G. Radocinski, G. K. Corlett, G. C. Hulley, S. G. Schladow, and T. E. Steissberg. 2009. Satellite observations indicate rapid warming trend for lakes in California and Nevada. *Geophys. Res. Lett.* **36**, L22402. doi:[10.1029/2009GL040846](https://doi.org/10.1029/2009GL040846)
- Schneider, P., and S. J. Hook. 2010. Space observations of inland water bodies show rapid surface warming since 1985. *Geophys. Res. Lett.* **37**: L22405. doi: [10.1029/2010GL045059](https://doi.org/10.1029/2010GL045059)
- Schwab, D. J., G. A. Leshkevich, and G. C. Muhr. 1999. Automated mapping of surface water temperature in the Great Lakes. *J. Great Lakes Res.* **25**: 468–481. doi:[10.1016/S0380-1330\(99\)70755-0](https://doi.org/10.1016/S0380-1330(99)70755-0)
- Serreze, M. C., M. M. Holland, and J. Stroeve. 2007. Perspectives on the Arctic's shrinking sea-ice cover. *Science* **315**: 1533–1536. doi:[10.1126/science.1139426](https://doi.org/10.1126/science.1139426)
- Smagorinsky, J. 1963. General circulation experiments with the primitive equations: I. The basic experiment\*. *Mon. Weather Rev.* **91**: 99–164. doi:[10.1175/1520-0493\(1963\)091<0099:GCEWTP>2.3.CO;2](https://doi.org/10.1175/1520-0493(1963)091<0099:GCEWTP>2.3.CO;2)
- Straile, D., K. Jöhnk, and R. Henno. 2003. Complex effects of winter warming on the physicochemical characteristics of a deep lake. *Limnol. Oceanogr.* **48**: 1432–1438. doi:[10.4319/lo.2003.48.4.1432](https://doi.org/10.4319/lo.2003.48.4.1432)
- Sugiyama, N., S. Kravtsov, and P. Roebber. 2018. Multiple climate regimes in an idealized lake–ice–atmosphere model. *Clim. Dyn.* **50**: 655–676. doi:[10.1007/s00382-017-3633-x](https://doi.org/10.1007/s00382-017-3633-x)
- Toffolon, M., S. Piccolroaz, B. Majone, A. Soja, F. Peeters, M. Schmid, and A. Wüest. 2014. Prediction of surface temperature in lakes with different morphology using air temperature. *Limnol. Oceanogr.* **59**: 2185–2202. doi:[10.4319/lo.2014.59.6.2185](https://doi.org/10.4319/lo.2014.59.6.2185)
- Tulonen, T., P. Kankaala, A. Ojala, and L. Arvola. 1994. Factors controlling production of phytoplankton and bacteria under ice in a humic, boreal lake. *J. Plankton Res.* **16**: 1411–1432. doi:[10.1093/plankt/16.10.1411](https://doi.org/10.1093/plankt/16.10.1411)
- Van Cleave, K., J. Lenters, J. Wang, and E. Verhamme. 2014. A regime shift in Lake Superior ice cover, evaporation, and water temperature following the warm El Niño winter of 1997–98. *Limnol. Oceanogr.* **59**: 1889–1898. doi:[10.4319/lo.2014.59.6.1889](https://doi.org/10.4319/lo.2014.59.6.1889)
- Verburg, P., R. E. Hecky, and H. Kling. 2003. Ecological consequences of a century of warming in Lake Tanganyika. *Science* **301**: 505–507. doi:[10.1126/science.1084846](https://doi.org/10.1126/science.1084846)
- Vollmer, W., B. Joris, P. Charlier, and S. Foster. 2008. Bacterial peptidoglycan (murein) hydrolases. *FEMS Microbiol. Rev.* **32**: 259–286. doi:[10.1111/j.1574-6976.2007.00099.x](https://doi.org/10.1111/j.1574-6976.2007.00099.x)
- Wagner, C., and R. Adrian. 2009. Cyanobacteria dominance: Quantifying the effects of climate change. *Limnol. Oceanogr.* **54**: 2460–2468. doi:[10.4319/lo.2009.54.6\\_part\\_2.2460](https://doi.org/10.4319/lo.2009.54.6_part_2.2460)
- Xue, P., C. Chen, P. Ding, R. C. Beardsley, H. Lin, J. Ge, and Y. Kong. 2009. Saltwater intrusion into the Changjiang River: A model-guided mechanism study. *J. Geophys. Res. Oceans* **114**: C02006. doi:[10.1029/2008JC004831](https://doi.org/10.1029/2008JC004831)
- Xue, P., D. J. Schwab, and S. Hu. 2015. An investigation of the thermal response to meteorological forcing in a hydrodynamic model of Lake Superior. *J. Geophys. Res. Oceans* **120**: 5233–5253. doi:[10.1002/2015JC010740](https://doi.org/10.1002/2015JC010740)
- Xue, P., J. S. Pal, X. Ye, J. D. Lenters, C. Huang, and P. Y. Chu. 2017. Improving the simulation of large lakes in regional climate modeling: Two-way lake–atmosphere coupling with a 3D hydrodynamic model of the Great Lakes. *J. Clim.* **30**: 1605–1627. doi:[10.1175/JCLI-D-16-0225.1](https://doi.org/10.1175/JCLI-D-16-0225.1)
- Zhong, Y., M. Notaro, S. J. Vavrus, and M. J. Foster. 2016. Recent accelerated warming of the Laurentian Great Lakes: Physical drivers. *Limnol. Oceanogr.* **61**: 1762–1786. doi:[10.1002/lno.10331](https://doi.org/10.1002/lno.10331)

#### Acknowledgments

This is contribution 47 of the Great Lakes Research Center at Michigan Technological University. The Michigan Tech high performance computing cluster, *Superior*, was used in obtaining the modeling results presented in this publication. Xue's research was supported by the National Aeronautics and Space Administration, grant#80NSSC17K0287. This is GLERL contribution number 1893.

#### Conflict of Interest

None declared.

Submitted 10 November 2017

Revised 24 February 2018

Accepted 06 September 2018

Associate editor: Francisco Rueda